ESTIMATION OF EARTHQUAKE-INDUCED SETTLEMENT OF CLAY LAYER

H. Matsuda [1], H. Sato [2], T.T. Nhan [3]

[1]*Professor, Yamaguchi University, hmatsuda@yamaguchi-u.ac.jp*
[2]*Professional Engineer, Coastal Engineering Division, Fukken Co., Ltd., h-sato@fukken.co.jp*
[3]*Doctor, University of Sciences, Hue University, Vietnam, ttnhan@hueuni.edu.vn*

Abstract

Based on the settlement-time records observed in Port Island, Kobe, Japan, the settlement of clay layer was confirmed to be affected by the Hyogo-ken Nanbu Earthquake 1995. So, to estimate the earthquake-induced settlement of clay layer, a lot of cyclic simple shear tests have been carried out on clays with different plasticity indices and an estimation method on the post-earthquake settlement was developed. In this study, to evaluate the applicability of this method, firstly under the undrained condition, undisturbed clay specimens which were taken from the alluvial clay layer at GL-18m beneath the river dike, were subjected to the multi-directional cyclic shear transformed from the acceleration-time histories recorded at the place close to the sampling site and the post-cyclic settlement was measured with time. Secondly, experimentally recorded settlements were compared with those of predicted one.

The undisturbed specimen was taken from the alluvial clay layer beneath the Kyuukitakami river dike which is located in Ishinomaki, Japan (hereinafter call it as Tohoku clay). Physical properties of Tohoku clay are ρ_s: 2.607g/cm^3, w_L:124.7%, w_P:40.5%, I_P:84.2, C_c:1.29. In this study, multi-directional cyclic simple shear test apparatus was used. In the experiments, after the consolidation under in situ overburden pressure of 157kPa, the specimen was subjected to the cyclic shear strains transformed from the earthquake-induced acceleration-time histories including EW and NS components. After undrained cyclic shear, the drainage from top surface of the specimen was permitted and the settlement and the excess pore water pressure at the bottom surface were measured with time.

In conclusion, the prediction method for the post-earthquake settlement was shown and by comparing the experimentally obtained settlement with the calculated one, the applicability of this method was investigated. Although the predicted results have a tendency to overestimate, the prediction method shown in this study would be useful as a preliminary prediction of the post-earthquake settlement of clay layer.

Keywords: settlement; clay; earthquake

1. Introduction

When the loose sand layer placed below the ground water table is subjected to the strong earthquake-induced cyclic shear, the sand layer might liquefy and the structures on the ground surface would be seriously damaged. For the clay layer, when the excess pore water pressure is generated under the strong earthquake and increased close to the confining pressure, the horizontally piled clay layer does not suffer from a serious damage due to the cohesion but the long term additional ground subsidence would occur by the dissipation of the excess pore water pressure. Such a subsidence has been confirmed at the Mexico earthquake 1957 [1], Miyagiken-oki earthquake 1978 [2] and Hyogo-ken Nanbu earthquake (hereinafter called as Kobe Earthquake) 1995 [3]. At Port Island which is the artificially reclaimed island near the city center of Kobe, Japan, after Kobe Earthquake, as an instantaneous settlement, the ground subsidence of about 26cm was observed and the differential settlement between buildings and the surrounding ground seriously affected the lifelines. The depth of the original seabed was 10-13m and the alluvial clay layer of 10-20m thick (called as Ma13) lies beneath the reclaimed stratum and underlain by the Pleistocene laminated gravel and sand layers which sandwich the thin silt and clay layers. The upper part of the gravel and sand layers permits the drainage from Ma13 and sustains the pile load. When Kobe Earthquake occurred on 17 January, 1995, the second reclamation works at the south part of Port Island have almost completed and at 928days before the earthquake the settlement monitoring started at the ground surface, the bottom of the alluvial clay layer (Ma13) and the Pleistocene clay layers (Ma12 and Ma9), and also sequentially continued after the earthquake.

Fig.1 shows the settlement-time curves in which symbol ● shows the settlement at the ground surface, and the symbol ○ shows those of the settlement gauge placed at the bottom surface of the Alluvial clay layer (Ma13). The curve ③ shows a difference between the settlement-time curves of the symbols ● and ○. The instantaneous settlement of about 26cm which is caused mainly at the reclaimed fill is seen just after the earthquake and the settlement is continuously increasing after the earthquake. The curve ① shows the predicted result by the hyperbolic curve method for the case of no earthquake and the curve ② was obtained
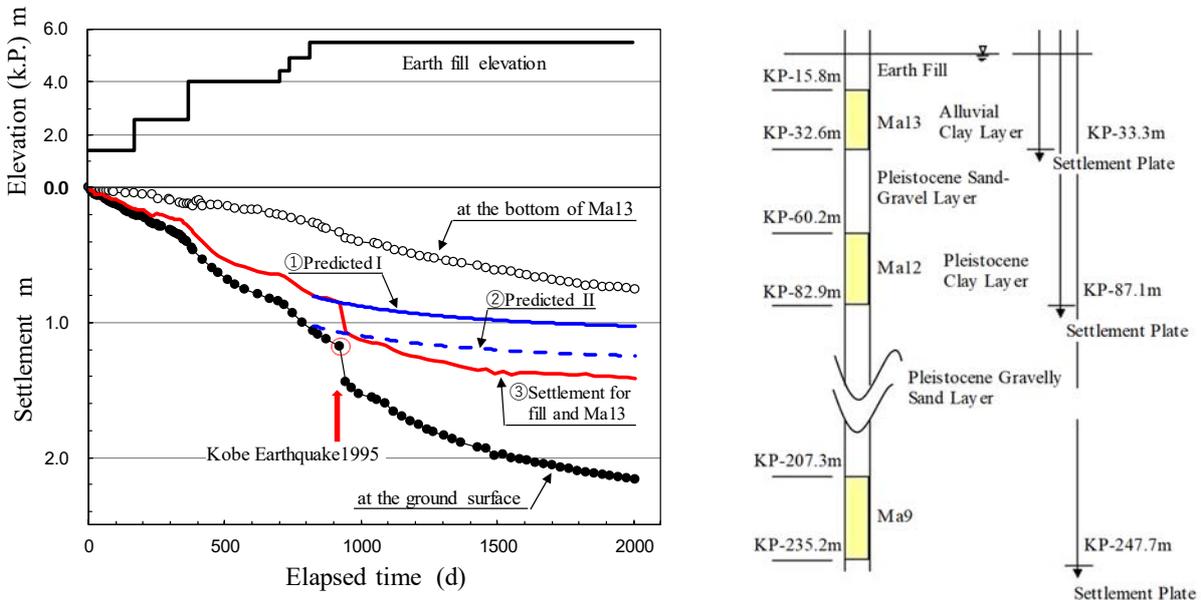

Fig. 1 – Differential settlement at the ground surface and the bottom surface of the alluvial clay layer, sequentially measured before and after the Kobe Earthquake 1995 [4, 5, 6]

2

by moving the curve ① down to the first data point after the earthquake. The difference between the curve ② and ③ is considered to be affected by the earthquake. The alluvial clay layer Ma13 was improved by the sand drain method in which the diameter of sand pile was 50cm and the pile spacing was 2.5m and 3.0m. By using the Barron's equation, the difference between curve ② and curve ③ was estimated as 10.3cm at the time of the degree of consolidation 90% and those containing the secondary consolidation was also estimated as 17.0cm. These values mean that the settlement-time curve of clay layer is affected by the earthquake-induced ground motions.

After Kobe Earthquake, to estimate the earthquake-induced settlement of clay layer, a lot of cyclic simple shear tests have been carried out on clays including different plasticity indices and a prediction method on the post-earthquake settlement was developed. In this study, to evaluate the applicability of this method, firstly under the undrained condition, undisturbed clay specimen which was taken from the alluvial clay layer at GL-18m beneath the river dike, was subjected to the multi-directional cyclic shear transformed from the acceleration-time histories recorded at the place close to the sampling site and the post-cyclic settlement was measured with time. Secondly, experimentally recorded settlements were compared with those of predicted one.
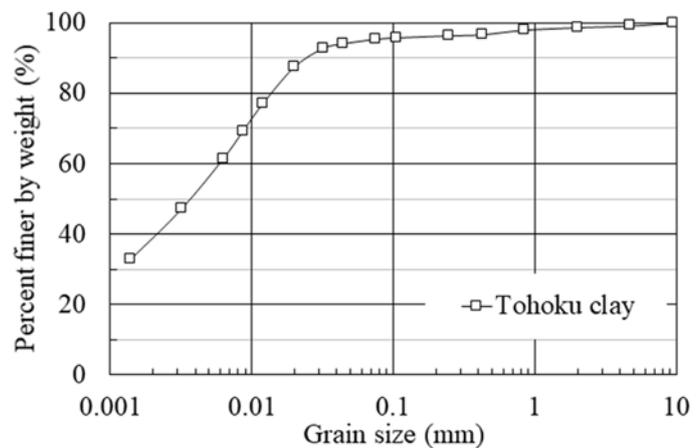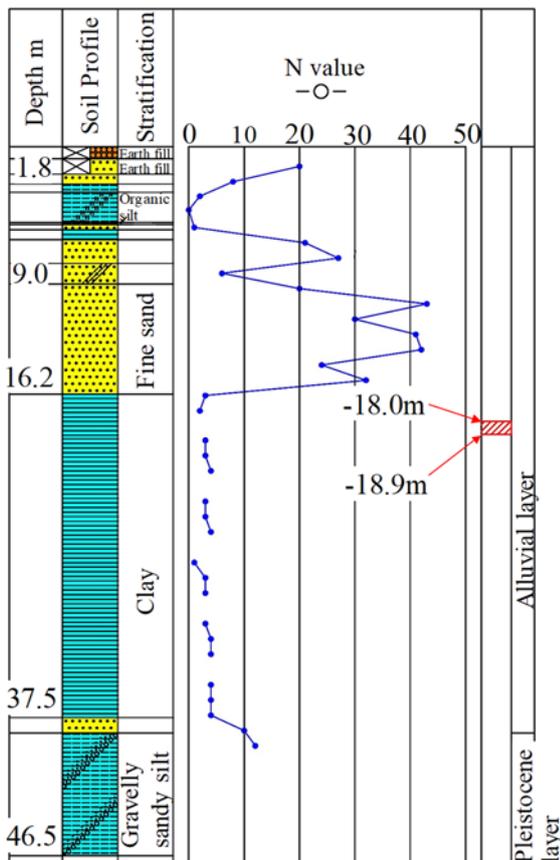
Fig. 2 – Soil profiles in which the undisturbed sample was taken from the alluvial clay layer at a depth of GL-18.0m

Fig. 3 – Particle size distribution curve on Tohoku clay

3

2. Undrained multi-directional cyclic shear tests on undisturbed clay

2.1 Sample

The sample used in this study was taken from the alluvial clay layer which is shown in Fig.2, at GL-18m beneath the Kyuukitakami river dike in Ishinomaki City, Miyagi, Japan. The undisturbed sample was pushed out from the thin wall tube sampler and cut with the predetermined length. The particle size distribution curve of the sample and the physical properties are shown in Fig.3 and Table 1. In the experiments, the undisturbed sample and the reconstituted sample which are called as undisturbed Tohoku clay and disturbed Tohoku clay, respectively, were used. The disturbed specimen was made from the undisturbed one by mixing with the de-aired water to form a slurry having the liquid limit of 150%. The slurry was de-aired in the vacuum cell and poured into the shear box.

2.2 Apparatus and test procedures

Strain-controlled uniform or irregular cyclic shear strain was applied to the specimen by the multi-directional cyclic simple shear test apparatus [7]. The dimension of specimen is 20mm in height and 75mm in diameter and the specimen was subjected to the cyclic shear strains from the orthogonal direction, independently.

The test procedure is as follows. For both the undisturbed and disturbed specimens, after the completion of pre-consolidation under the in situ vertical effective stress ($p'_c = 157$ kPa), the cyclic shear tests were carried out under the undrained condition and the change of the excess pore water pressure was measured with time. For the case of uniform cyclic shear tests, the wave forms which was applied from the orthogonal directions are sinusoidal with the period of 2.0s and the shear strain amplitude was changed in the range from 0.12% to 3.05%. The phase difference θ of strain waves applied from the two orthogonal directions and the number of cycles n were set as $\theta=90°$ and $n=200$, respectively. In the series of cyclic shear tests, the irregular cyclic shear wave form which was transformed from the acceleration records obtained at the 2011 off the Pacific coast of Tohoku Earthquake was used.

Table 1 – Physical properties of Tohoku clay

	Particle density ρ_s (g/cm^3)	Liquid limit w_L (%)	Plastic limit w_P (%)	Plasticity index I_p	Compression index C_c
Tohoku clay	2.607	124.7	40.5	84.2	1.29

After the undrained cyclic shear, the drainage from the top surface of the specimen was allowed and the settlement of the specimen was measured with time until the excess pore water pressure at the bottom surface of the specimen dissipated. For the case of the undisturbed specimen, the consolidation tests were continued under the step loading as $\sigma_v = 294 kPa$, $\sigma_v = 392 kPa$. The experimental patterns are shown in Table 2.

3. Effects of sample disturbance on the post-cyclic shear-induced settlement

3.1 Excess pore water pressure induced by undrained cyclic shear

Several researches about the cyclic shear-induced excess pore water pressure on saturated clays have been carried out, in which by using the strain controlled uni-directional cyclic simple shear test apparatus, Ohara et al. [8] found the hyperbolic relationships between the excess pore water pressure and the number of strain cycles. Later, Matsuda et al. [9] and Sato et al. [10] developed the following equation which includes the effects of cyclic shear direction, shear strain amplitude and number of strain cycles.

$$\frac{U_{dyn}}{\sigma'_{vo}} = \frac{G^*}{\alpha+\beta\cdot G^*} \tag{1}$$

4

Table 2 – List of cyclic shear tests applied to the undisturbed and disturbed specimens

Specimen	Cyclic shear wave form	Shear strain amplitude γ (%)	σ'_{v0} (kPa)	Number of cycles n	Phase difference θ (°)	After cyclic shear σ'_{v0} (kPa)
Un-disturbed	Uniform	0.13	157	200	90	294,392
		0.55				
		1.12				
		3.05				
	Irregular	The Tohoku Earthquake 2011				
Disturbed	Uniform	0.12	157	200	90	–
		0.45				
		0.90				
		2.86				

where U_{dyn} is the excess pore water pressure, σ'_{vo} is the initial effective stress, G^* is the cumulative shear strain defined as follows,

$$G^* = \sum \Delta G^* = \sum \sqrt{\Delta \gamma_x^2 + \Delta \gamma_y^2} \tag{2}$$

where, α and β are the experimental parameters and related to the shear strain amplitude as follows.

$$\alpha = A \cdot \gamma^m \tag{3}$$

$$\beta = \frac{\gamma}{B + C \cdot \gamma} \tag{4}$$

$$\gamma > -\frac{B}{C} \tag{5}$$

where $\Delta \gamma_x$ and $\Delta \gamma_y$ in Eq.(2) are the increment of shear strain in X direction and Y direction on the horizontal plane. γ is the shear strain amplitude, and A, B, C and m are the experimental constants. When the phase difference of the sinusoidal wave is set as $\theta = 90°$, G^* is obtained by Eq.(6) as a function of the number of cycles n and shear strain amplitude γ .

$$G^* = n \cdot (5.995 \cdot \gamma + 0.3510) \tag{6}$$

Fig.4 shows the change of excess pore water pressure with number of cycles n on undisturbed and disturbed Tohoku clay specimens. It is seen that the excess pore water pressure on the disturbed sample is larger than those of undisturbed one. This is considered due to the degradation of the soil structure by the disturbance. Fig.5 shows relationships between the excess pore water pressure ratio and G^* for undisturbed and disturbed samples. Plots in the figure are observed results and by which, it is possible to find the
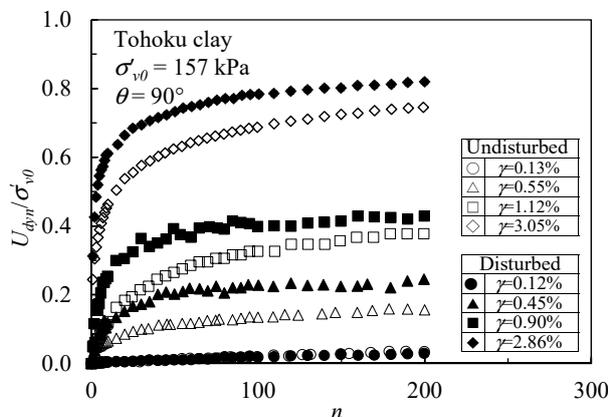

Fig. 4 – Relationships between U_{dyn}/σ'_{vo} and the number of cycles n on the undisturbed and disturbed samples
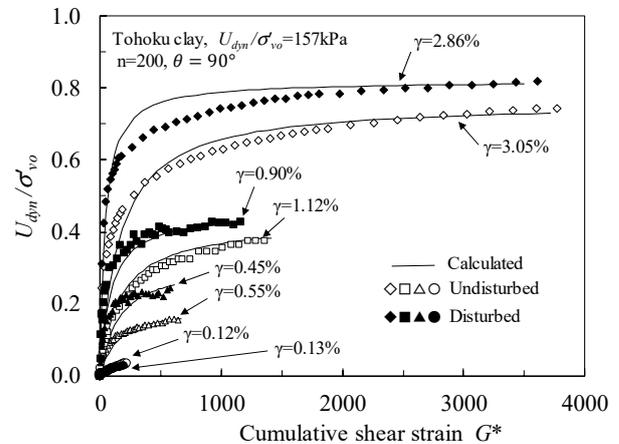
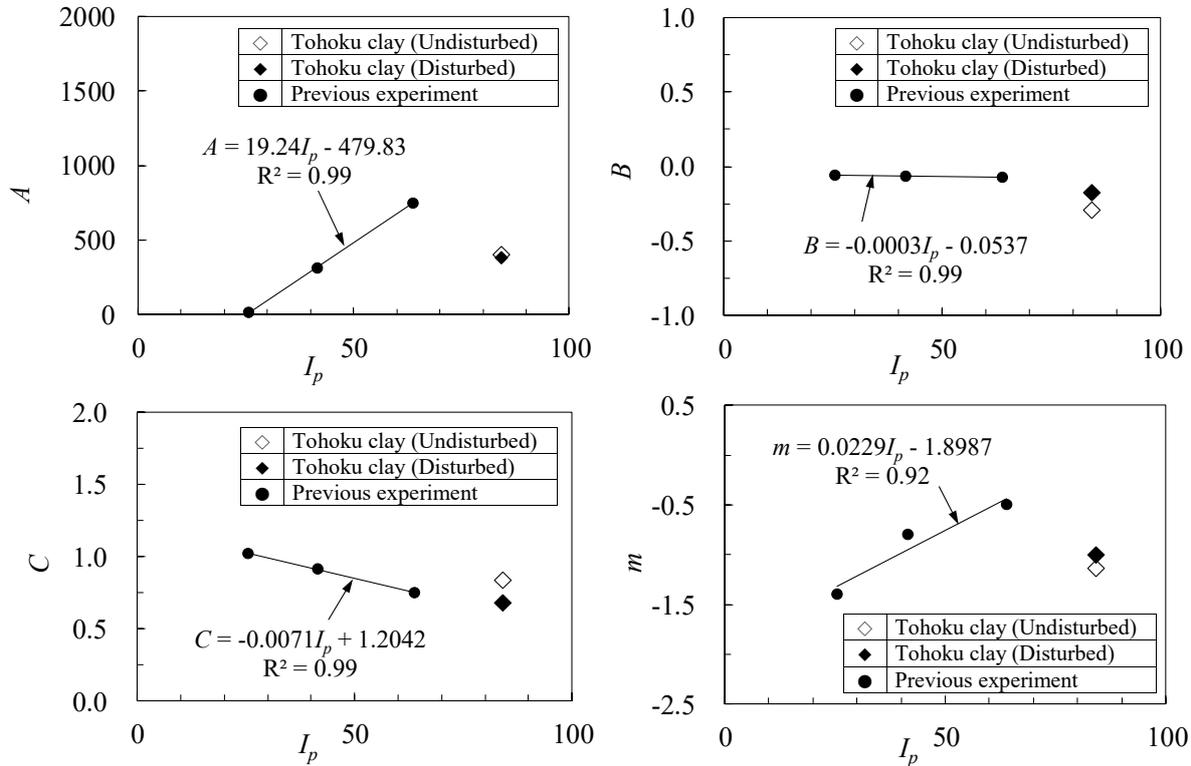Fig. 5 – Relationships between U_{dyn}/σ'_{vo} and the cumulative shear strain amplitude G^*[11]

5

Fig. 6 – Relationships between experimental constants A, B, C and m in Eqs.(3), (4) with the plasticity index of clay soil

experimental constants A, B, C and m in Eqs.(3) and (4). In Fig.5, the lines show the calculated ones by Eq.(1). Reasonable agreements between the observed and the calculated results are seen and this means that Eq.(1) is applicable to the undisturbed and disturbed specimen. For the low confinig stress as $\sigma'_{vo} = 49kPa$, the relationships between these experimental constants and the plasticity indicies have been observed for clays with different plasticity indicies as I_p=25.5, 41.6 and 63.8 [12] and the following relations were obtained.

$$A = 19.24 \cdot I_p + 479.8 \tag{7}$$

$$B = -0.0003 \cdot I_p - 0.0537 \tag{8}$$

$$C = -0.0071 \cdot I_p + 1.204 \tag{9}$$

$$m = 0.0229 \cdot I_p + 1.899 \tag{10}$$

Fig.6 shows the relationships between the experimental parameters A, B, C and m and the plasticity indices. For the results obtained under the relatively low confining stress, reasonable agreements between observed results and the fitted lines obtained by Eqs.(7), (8), (9), and (10) are seen. In Fig.6, the results for the undisturbed and disturbed Tohoku clay specimen are also shown.When comparing the experimental constants A, B, C and m with the fitted lines, for B and C by which the maximum value of U_{dyn}/σ'_{vo} is evaluated, reasonable tendencies with Eqs.(8) and (9) are shown. For constants A and m, however, which relating the initial gradients of the curve on U_{dyn}/σ'_{vo} - G^*, the tendencies are different from the Eqs.(7) and (10). Although this is considered due to the difference of confining stress, as shown later, when predicting the post earthquake settlemet of clay layer, because only the maximum value of U_{dyn}/σ'_{vo} is used, the effect of these differences would be minimized.

6

3.2 Cyclic shear-induced settlement of clay

As mentioned above, since the cyclic shear-induced settlement of clay layer is significantly related to the excess pore water pressure induced during the undrained cyclic shear, the settlement in strain which is the same as the volumetric strain under the K_o condition is obtained by the following equation [8].

$$\varepsilon_v = \frac{C_{dyn}}{1+e_o} log(SRR) \tag{11}$$

where C_{dyn} is the cyclic recompression index, e_o is the initial void ratio and SRR is the stress reduction ratio which is defined as follows.

$$SRR = \frac{1}{1-\frac{U_{dyn}}{\sigma'_{vo}}} \tag{12}$$

Fig.7 shows the cyclic shear-induced settlement–time relations on undisturbed and disturbed Tohoku clay. For the case of the shear strain amplitude as 3.05% and 2.86%, it is seen that the rate of consolidation is faster in the undisturbed specimen than disturbed one. This is considered due to that the part of soil particle structure still remains. After the end of primary consolidation, settlement increases linearly with the logarithm of time, i.e. the secondary consolidation occurs even for the small shear strain amplitude.

Relationships between Δe and SRR on the undisturbed and disturbed Tohoku clay are shown in Fig.8. It is seen that Δe increases linearly with SRR and the gradients of these lines show the cyclic recompression index C_{dyn}. Similar relations for the cyclic recompression index C_{dyn} were observed on clays with I_p=25.5, 41.6 and 63.8 and a following equation was derived.

$$C_{dyn} = 0.0019 \cdot I_p + 0.0202 \tag{13}$$

Results of C_{dyn} on undisturbed and disturbed Tohoku clay are shown in Fig.9 together with those on clays with different I_p and lines calculated by Eq.(13). Plots of Tohoku clay specimen are on the line extrapolated from the previous experimental results. This shows that Eq.(13) is possible to apply for a wide range of plasticity indices including undisuturbed and disturbed specimen.
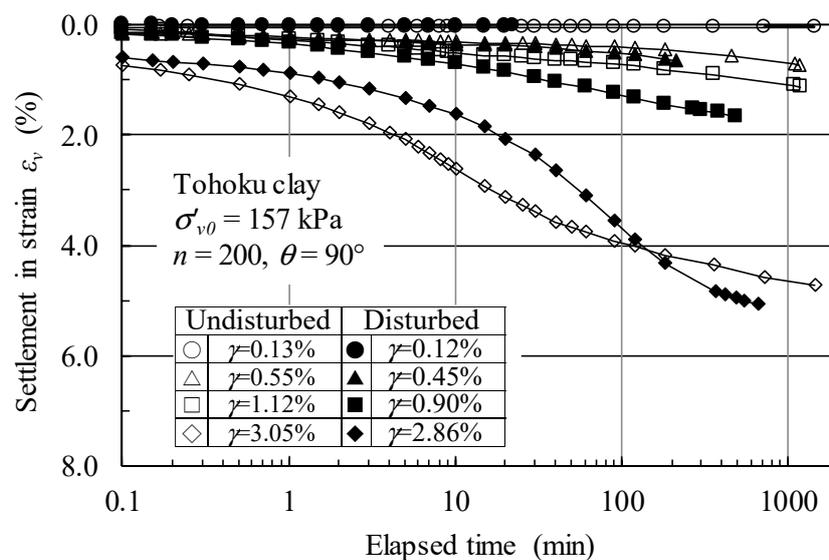

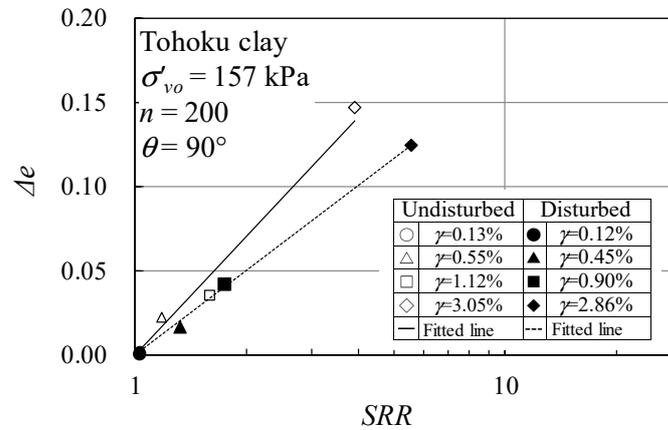Fig. 7 – Cyclic shear-induced settlement-time relations on undisturbed and disturbed Tohoku clay.

7

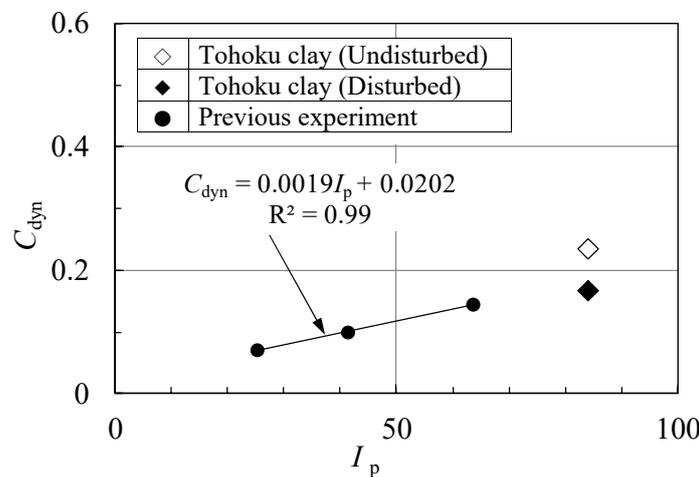Fig. 8 – Relationships between Δe and *SRR* for undisturbed and disturbed Tohoku clay

Fig. 9 – Prediction of C_{dyn} in relation with the plasticity index of clay

4. Application of prediction method on the post earthquake settlement of caly layer

4.1 Experimental simulation on the cyclic shear-induced settlement of clay layer by the Tohoku Earthquake 2011

In this study, to confirm the applicability of the prediction method on the post-earthquake settlement of clay layer, firstly after the preconsolidation under in situ overburden pressure of 157kPa, the undisturbed Tohoku clay specimen was subjected to the irregular cyclic shear strains transformed from the acceleration-time histories of EW and NS components recorded at the 2011 off Pacific coast of Tohoku Earthquake [14] and the post-cyclic settlement was measured with time. Secondly, experimentally recorded settlements were compared with predicted results.

Fig.10 shows the time histories of shear strain at GL-20m of the sampling site calculated by using FLIP program [13]. The acceleration-time histories were recorded at Ishinomaki Fishing port which is about 2km far from the sampling site [14]. Although the position of the seismometer is not the same as the sampling site, since the soil profiles in both places are confirmed to be relatively similar, effects of the difference of the ground condition is considered to be minimized. In the shear strain-time histories for NS and EW in Fig.10, the first and the second portions which show a relatively large shear strain amplitude, are seen at the time of around 40s and 90s and such wave patterns are known due to the effects of epicenters of the earthquake. As
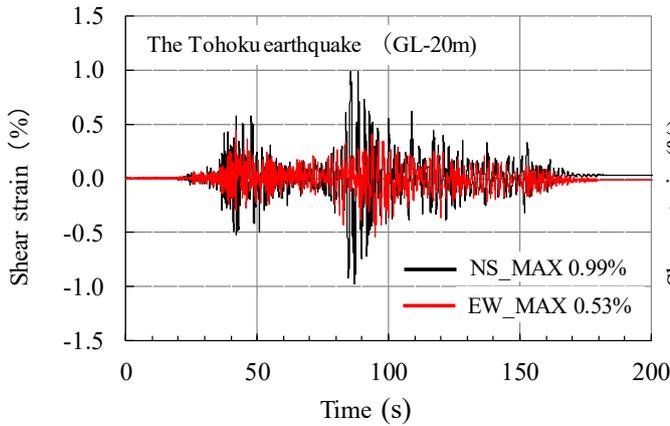
8

Fig. 10 – Time histories of shear strain at GL-20m of the sampling site calculated by FLIP program from the transferred acceleration records. These shear waves were used as input data in the cyclic shear tests
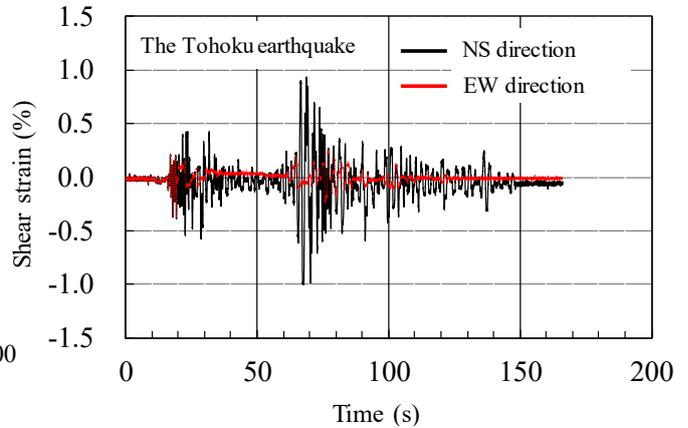

Fig. 11 – Shear strain - time relations recorded in the cyclic shear test

for the maximum shear strain amplitude for NS and EW components, γ_{maxNS} =1.0% and γ_{maxEW} =0.5% are obtained.

When shear strain waves were applied to the servo system in the multi-directional cyclic shear test apparatus, by measuring the shear deformation of the specimen, the shear strain-time histories were recorded as in Fig.11. When comparing Fig.10 with Fig.11, it is seen that input shear strain waves are applied to the specimen precisely.

The accumulation process of the excess pore water pressure induced by the irregular cyclic shear is shown in Fig.12. It is seen that U_{dyn}/σ'_{vo} increases stepwise due to the first and second part with larger shear strain amplitude as shown in Fig.11 and reached up to U_{dyn}/σ'_{vo}=0.13. Relationships between the settlement in strain ε_v and the elapsed time are shown in Fig.13 and the final settlement at the time of 1,440min reaches to ε_v =0.61%. This value means that the settlement of the alluvial clay layer with the thickness of 21m as shown in Fig.2 reaches 13cm.
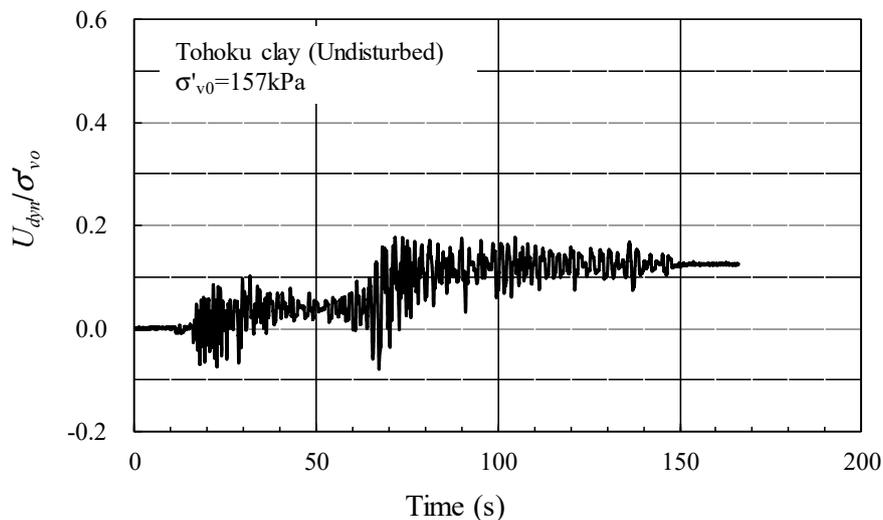

Fig. 12 – Excess pore water pressure induced by the irregular cyclic shear
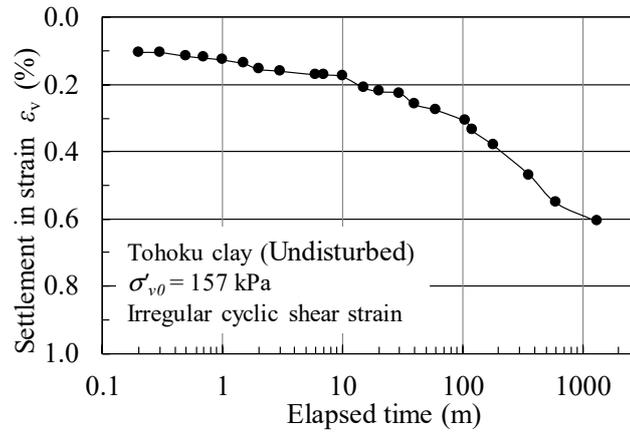
9

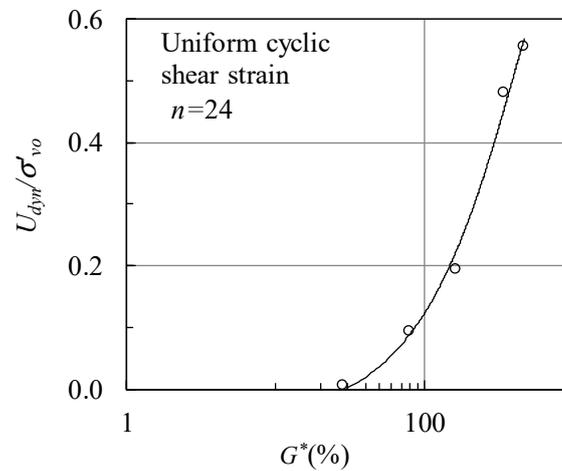Fig. 13 – Irregular cyclic shear-induced settlement of undisturbed specimen

Fig. 14 – Relationships between U_{dyn}/σ'_{vo} and G^* induced by the uniform multi-directional cyclic shear at the number of strain cycles *n*=24

4.2 Converting the irregular cyclic shear to the equivalent uniform cyclic shear

To predict the cyclic shear-induced excess pore water pressure and the post-earthquake settlement, Eqs.(1) and (11) were used. In this study, by predicting the settlement-time relation as shown in Fig.13 which was observed by the irregular cyclic shear on the undisturbed sample, the applicability of the proposed method was investigated.

When predicting the earthquake-induced settlement of clay layer, firstly, it is necessary to convert the irregular cyclic shear to the equivalent uniform cyclic shear strain amplitude and the number of cycles [15]. The equivalent number of cycles N_{cy} is calculated by Eq.14.[10, 16]

$$N_{cy} = \frac{1}{2}\sum_{i=1}^{2T_n}\left(\frac{u_i}{u_{max}}\right)^2 \tag{14}$$

where u_i is the amplitude of i-th half cycle, u_{max} is the maximum amplitude in all half cycles and T_n is the total number of cycles. By applying Eq.14 to the shear strain time histories, $N_{cy} = 24$ was obtained. Secondly, to find the equivalent uniform cyclic shear strain amplitude, relationships between the excess pore water pressure ratio at the number of cycles $n = N_{cy} = 24$ and the cumulative shear strain amplitude for the uniform shear waves G^* are shown as Fig.14. In the case of irregular cyclic shear, the excess pore water pressure increased up to $U_{dyn}/\sigma'_{vo} = 0.13$ as shown in Fig.12, then from Fig.14, the value of G^* is obtained as 100.6%.
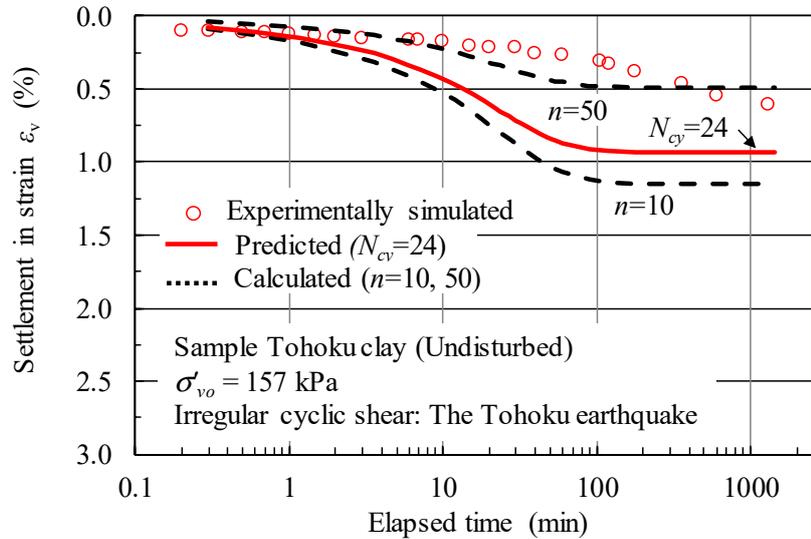
10

4d-0007

Fig. 15 – Experimentally simulated and predicted settlement-time relations

Thirdly, in Eq.(6) by applying G^*=100.6% and n=24, equivalent uniform shear strain amplitude γ_{eq} is derived as $\gamma_{eq} = 0.64\%$, and since γ_{maxNS} was shown as 1.0% in Fig.11, $\gamma_{eq}/\gamma_{maxNS} = 0.64$ is obtained. This value is close to the one obtained by using the equation proposed by Matsuda et al. [15].

4.3 Applicability of the prediction method on the earthquake-induced settlement of clay layer

The applicability of the prediction method of earthquake-induced settlement of clay layer was preliminary confirmed by comparing the predicted settlemen-time curve with those for the experimental simulation on the undisturbed Tohoku clay. The experimental constants used in the equations were predicted in relation to the plasticity index I_p of the soil. In the case of Tohoku clay, since I_p =84.2 is obtained as shown in Table 2, experimental constants are obtained by Eqs.(7)-(10) and Eq.(13) and also referencing Figs.6 and 9. As for the equivalent number of cycles N_{cy}=24, however, which was obtained for the shear strain waves concerned, because the predicted results are affected by the number of cycles, in this study, by obtaining the results for the number of cycles with 10 and 50, and then interporated to N_{cy}=24. Fig.15 shows experimentally simulated and predicted settlement-time relations in which the effect of the coefficient of consolidation are included. It is seen that the predicted settlement in strain as 0.93% is larger than the experimentally simulated one as 0.61% and the time to the end of primary consolidation (EOP) is relatively short in the predicted result. So, when comparing the predicted results with the experimentally simulated ones on the settlement-time relation, although the prediction method overestimates the settlement due to that the settlement of Tohoku clay is very small, the estimation method shown in this study would be useful preliminarily.

5. Conclusions

In this study, the estimation method for the post-earthquake settlement was shown and by comparing the experimentally obtained settlement with the predicted one, the applicability of this method was investigated. The main conclusions are as follows.
1) In the experimental constants A, B, C and m, reasonable tendencies for B and C are obtained by Eqs.(8) and (9). For constants A and m, however, the tendencies are different from the Eqs.(7) and (10). When estimating the post-earthquake settlement of clay layer, because the maximum value of U_{dyn}/σ'_{vo} is decided by B and C, the effect of A and m would be minimized.
2) For the cyclic recompression index C_{dyn}, Eq.(13) is possible to apply for the wide range of plasticity indices including undisuturbed and disturbed specimen.
3) The equivalent number of cycles N_{cy} and the equivalent uniform shear strain amplitude γ_{eq} were obtained.

11

4) Although the predicted results have a tendency to overestimate, the prediction method shown in this study would be useful as a preliminary prediction of the post-earthquake settlement of clay layer.

6. Acknowledgements

7. References

[1] Zeevaert L. (1983): Foundation engineering for difficult subsoil conditions. *Van Nostrand Co. Ltd*, 2nd edition.

[2] Suzuki T. (1984): Settlement of saturated clays under dynamic stress history. *Journal of the Japan Society of Engineering Geology*, 25 (3), 21-31. (in Japanese)

[3] Matsuda H. (1997): Estimation of post-earthquake settlement-time relations of clay layers. *Journal of JSCE Division* C, 568 (III-39), 41-48. (in Japanese)

[4] Department of Urban Development. (1995): *Report on ground deformation of reclaimed land due to Hyogo-ken Nanbu earthquake*, *Kobe city*. (in Japanese)

[5] Matsuda H. (1997): Estimation of post-earthquake settlement-time relations of clay layers. *Journal of JSCE Division C*, 568(III-39), 41-48. (in Japanese)

[6] Nhan TT., Sato H., Matsuda H., Huong HTS., Thien ĐQ., Tin TN. (2018): Effects of multi-directional cyclic shear on the secondary consolidation of saturated clay. *Eleventh U.S. National Conference on Earthquake Engineering*, TT-024, 987, 10pages.

[7] Matsuda H., Nhan T. T., Sato H. (2017): Effects of cyclic shear direction on earthquake-induced pore water pressure and settlement of clay layer. *16WCEE 2017*, Paper # 1483.

[8] Ohara, S., Matsuda, H. (1988): Study on the settlement of saturated clay layer induced by cyclic shear. *Soils and Foundations*, 28(3), 103-113.

[9] Matsuda, H., Nhan, T.T., Ishikura, R. (2013): Prediction of excess pore water pressure and post-cyclic settlement on soft clay induced by uni-directional and multi-directional cyclic shears as a function of strain path parameters. *Soil Dynamics and Earthquake Engineering*, 49, 75-88.

[10] Sato H., Nhan TT., Matsuda H. (2018): Earthquake-induced settlement of a clay layer. *Soil Dynamics and Earthquake Engineering* 104, 418–431.

[11] Matsuda H., Nhan TT., Sato H., Hara H.(2018): Multi-directional cyclic shear induced pore pressure and settlement of undisturbed clay. *Eleventh U.S. National Conference on Earthquake Engineering*, TT-024, 967, 10pages, 2018.

[12] Nhan, T. T., Matsuda, H., Sato, H. (2017): A model for multi-directional cyclic shear-induced pore water pressure and settlement on clays, *Bulletin of Earthquake Engineering*, 15, 7, 2761-2784.

[13] Iai, S., Matsunaga, Y., Kameoka, T. (1990): Strain space plasticity model for cyclic mobility. *Report of the Port and Harbour Research Institute*, 29, 4, 27-56.

[14] Saeki K., Sato H., Nishimoto A., Fujii T., Umezu T., Asakawa N., Mikami N. (2013): Ex post facto estimation of the damage of quay walls caused by ground motion of the 2011 off the Pacific Coast of Tohoku Earthquake. *Journal of JSCE Division* B3, 69, 2, I_281-I_286. (in Japanese)

[15] Matsuda H., Hoshiyama E. (1992): Uniform strain series equivalent to seismic strain. *10WCEE*, 1329-1334.

[16] Malhotra PK. (2002): Cyclic-demand spectrum. *Earthq Eng Struct Dyn*, 31:1441–57.